Journal of Visualization, Vol. 4, No. 2 (2001) 131-138

PSP Measurement of Flow Fields in a Supersonic Combustor with a Backward-facing Step

Matsumoto, M.*[1], Tomioka, S.*[2] and Ikeda, Y.*[3]

*1 4-16-2-201 Nagamachiminami Taihaku-ku Sendai 982-0012, Japan.
*2 National Aerospace Laboratory, Kakuda Research Center, Kakuda, Miyagi 981-1525, Japan.
*3 Department of Mechanical Engineering, Kobe University, Nada, Kobe 657-8501, Japan.

Received 30 November, 2000.
Revised 2 March, 2001.

***Abstract*:** The mixing fields within a SCRAM-jet combustion chamber are visualized using pressure-sensitive paint (PSP) as an oxygen sensor. The experiments are performed in a small supersonic wind tunnel at the National Aerospace Laboratory - Kakuda Research Center (NAL-KRC). The main stream Mach number is 2.4, and the dynamic pressure ratios between the injected gas and the main flow are 0.3, 0.7, 1.1 and 1.5. Three fuel injection nozzles are used; oxygen is injected from the central nozzle and air from the two nozzles at either side. The spread of the injected gas is measured to observe the effects of placing the nozzles in different positions. The results show that the jet has its own independent flow structure, and that little mixing of gases occurs between the flow structures created by each nozzle. When the injection dynamic pressure ratio is increased, the oxygen fraction rises in the recirculation zone and falls in the separation zone downstream of the injection.

***Keywords*:** pressure sensitive paint, SCRAM-jet, oxygen distributions, injection, backward-facing step.

1. Introduction

The SCRAM-jet engine is under consideration for use as a propulsion device for the next generation of space planes. The flow of air at the entrance to the SCRAM-jet combustor is maintained at supersonic speed to reduce both the pressure loss created by a shock wave and the load on the structure required to restore the temperature and pressure. Therefore, harsh ignition conditions (high velocity, low temperature, low pressure) are created within the combustor. The ignition limits restrict the operating range of the engine, particularly in low total temperature zones.

Tomioka et al. (1997) investigated the flow field in the combustion chamber of this type of SCRAM-jet engine. They studied the effects of the three-dimensionality of the flow field on the ignition limits, using a supersonic combustor with a backward-facing step and perpendicular injection nozzles. The results indicated that a complex flow field is generated downstream of the backward-facing step, as shown in Fig. 1. Methods such as PIV were used to elucidate the characteristics of the flow, but it was difficult to measure flow in the vicinity of the walls or in the recirculation zone downstream of the step (Ikeda et al., 1999).

In the present work, pressure-sensitive paints (PSPs) were used to measure the pressure distribution along the wall surfaces of the combustion chamber. PSPs have been introduced recently as a new system for measuring pressure (Handa et al., 1999; Engler et al., 1992; Crites, 1993). The paint is an oxygen sensor, and the resulting pressure distributions have been used as a method of flow visualization. In the present study, oxygen was substituted for some of the injection gas in the SCRAM-jet combustor. PSPs were then used to study the behaviour of the injection gas at the wall surfaces.

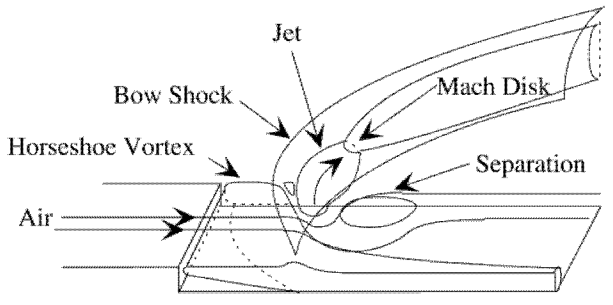

Fig. 1. Flow characteristics model behind backward-facing step.

2. Experimental Apparatus

The experiment was performed with a small supersonic wind tunnel at the National Aerospace Laboratory Kakuda Research Center (NAL-KRC). The test section used to model the supersonic combustor is shown in Fig. 2. The cross section of the test section was 94.3 mm × 51 mm and contained a 6 mm high (h) backward-facing step. Three supersonic injection-type fuel nozzles, 6 mm in diameter and 30 mm apart, were located 24 mm ($4h$) downstream from the backward-facing step. Air and oxygen were used in the nozzles to accommodate the PSPs.

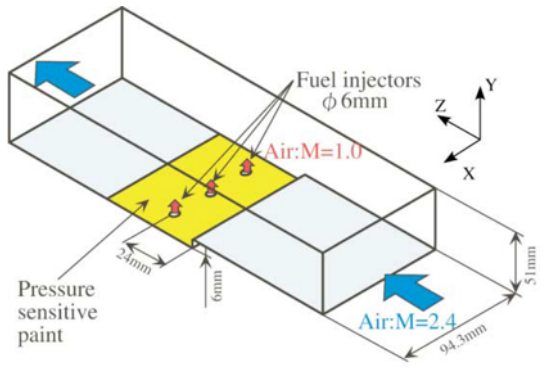

Fig. 2. Test section with backward-facing step and PSP sheet.

Ru(bpy) was used as the PSP dye molecule, and a TLC sheet was used as a binder. The Ru(bpy) was adsorbed onto the TLC sheet (silica gel 60) using ethyl alcohol as a solvent, and thoroughly dried before the sheet was pasted into the test section. An observation window for the PSP measurement was located on the upper surface of the test section, and LED lamps for PSP excitation were attached to windows set into the sides of the section. Two LED lamps were used, each consisting of 222 lamps with a peak wavelength of 460 nm (Nichia Corporation NSPB300A), thereby assuring adequate light for measurements.

A Hamamatsu Photonics CCD camera, C4742-95-12NR with 1024 × 1024 pixel resolution, was used to capture the images. Each pixel was capable of recording in 12 bits. The measurement configuration is shown in Fig. 3.

In addition, 21 gas-sampling holes (7 for each injector), 1 mm in diameter, were provided on the nozzle axis (x = 0 mm, ±30 mm). These were used for the *in situ* corrections. The pressure and oxygen fraction during the operation of the wind tunnel were measured.

3. Measurement of the Oxygen Distributions in the Vicinity of the Wall Surface

3.1 PSP and Measurement Principles

PSP uses collisional quenching, in which a dye is activated by a particular wavelength light, gives off fluorescence and phosphorescence and returns to its non-radiating base state when it collides with oxygen molecules. This

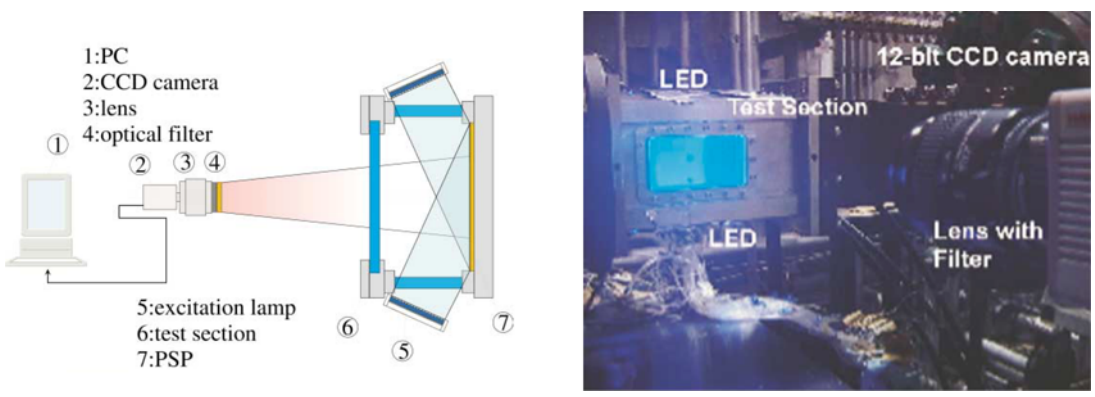

Fig. 3. PSP measurement configuration.

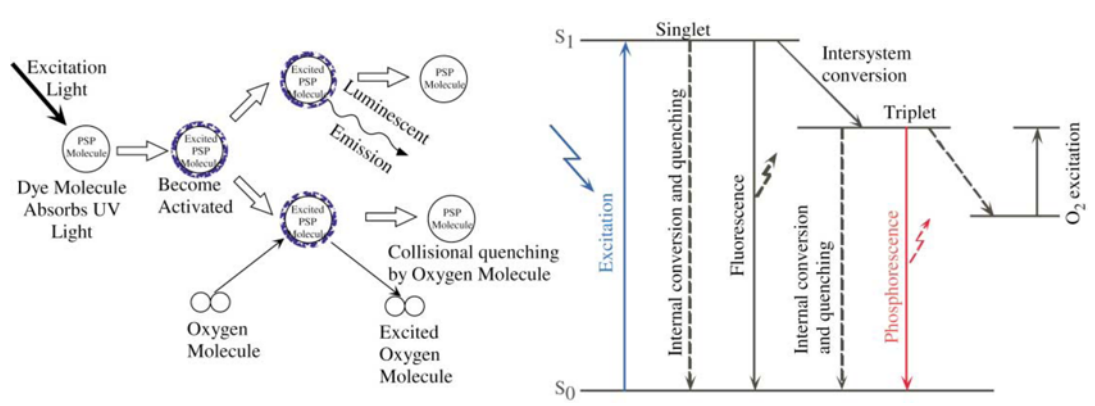

Fig. 4. Principle of PSP technique.

process is shown in Fig. 4. The Ru(bpy) used in the present experiment is excited by 457 nm light, and emits 600 nm light to return to its base state. But when there is a heavy collision with oxygen molecules under high pressure, when the concentration of oxygen molecules increases, the non-radiating quenching increases; and the brightness of the luminescence drops. The emitted light intensity ratio is given by the Stern-Volmer equation.

$$\frac{I_0}{I} = 1 + KN_{(O_2)}$$

This equation can be normalized to a reference state (subscript r) by

$$\frac{I_r}{I} = \frac{1 + K \cdot N_{(O_2)}}{1 + K \cdot N_{(O_2)_r}} = A + B\frac{N_{(O_2)}}{N_{(O_2)_r}}$$

In wind tunnel experiments, the conditions prior to the start of the test (atmospheric pressure) are generally used as the basic state. The following equation, taking non-linearity into account, is used.

$$\frac{I_r}{I} = \sum A_n \left(\frac{N_{(O_2)}}{N_{(O_2)_r}} \right)^n \qquad n = 0, 1, 2, \cdots$$

Here, a separate measurement is required to obtain the corrective coefficient A_n.

3.2 Correction Method for Oxygen Fraction

Normally, either an *a priori* or *in situ* method of correction is used to obtain the pressure distributions from the light intensity emitted by the PSP.

In the *a priori* method, the oxygen fraction and temperature characteristics of the PSP are measured in advance. The correction curve is obtained and used to convert the light intensity measured in the experiment to

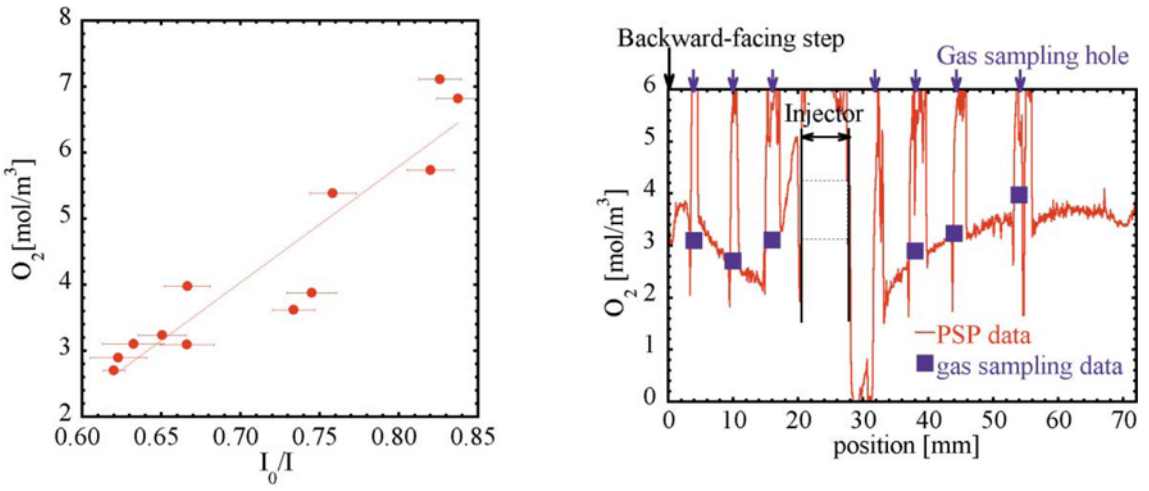

(a) PSP calibration curve

(b) Oxygen profile with gas sampling data

Fig. 5. PSP oxygen fraction profile.

oxygen distributions. The wall surface temperatures during the experiment are also measured, and used to correct the effect of temperature changes in the paint. For this reason, temperature sensitive paint (TSP) is often used in conjunction with PSP. However, the effects of dye deterioration cannot be ignored. This is caused when PSPs are exposed, such as in the present TLC-based PSP arrangement. The accuracy of the measurements will drop with time, even with temerature correction.

In the *in situ* method, a number of gas sampling ports are placed on the measuring surface and gas samples are taken during the experiment. The gas samples are analysed to obtain the oxygen concentration in the vicinity of the sampling ports. These measurements are compared with the light intensity emitted by the PSP, and a correction curve is obtained. This curve is then used to correct measurements on the entire surface. Using this method, it is relatively easy to obtain the pressure distributions, but the margin of error is large unless the wall surface is a uniform temperature since the proportional constants contained in the Stern-Volmer equation are temperature dependent. An aluminium plate was used as the TLC sheet in the present experiment. It was assumed that heat conduction through the metal plate provided a uniform temperature on the wall surface where measurements were taken. Therefore, the *in situ* method was used.

The calibration curve and the oxygen distributions above the side injection nozzles, obtained using the *in situ* method are shown in Figs. 5(a) and 5(b) for a dynamic pressure ratio of 0.3. The circle in Fig. 5(a) indicates the measured data and the line shows the calibration curve. Figure 5(b) shows the oxygen distribution from the recirculation zone upstream of the nozzle to the downstream separation zone. The squares on the graph indicate the oxygen concentration measured from the gas samples, and the line shows the oxygen distributions obtained using PSP as a function of distance from the backward-facing step. The oxygen fractions obtained from the PSP measurements are similar to those obtained from the gas samples, but there are some areas where they do not coincide. This is because the TLC adhesive layer often separates when processing the gas-sampling ports, and the PSP dye is not absorbed evenly in the vicinity of the gas sampling hole. Therefore, it is difficult to take accurate measurements of the emitted light intensity in the vicinity of the gas sampling holes. In addition, the PSP dye (Ru(bpy)) has a relatively large temperature dependency. However even with these problems, there is a correlation between the oxygen fractions obtained from gas samples and PSP.

4. Results and Discussion

The pressure distributions obtained without injected flow and with injected flow are shown in Figs. 6(a) and 6(b) respectively, for a dynamic pressure ratio of 0.7. The backward-facing step is located at the right side of the figures, and the main stream flows from right to left. The small black dots are the gas sampling holes, and the large black dots are the injection nozzles.

Without the injected flow, there was a low-pressure (separation) zone located downstream of the backward-facing step. The main flow reattached to the wall near the injectors, and the flow was homogeneous downstream from this points.

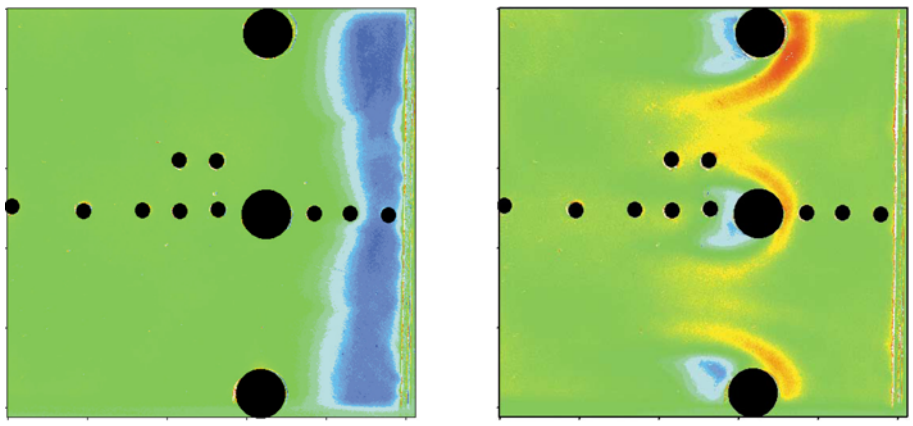

(a) Without injection (b) With injection

Fig. 6. Visualized pressure distributions of dynamic pressure ratio 0.7.

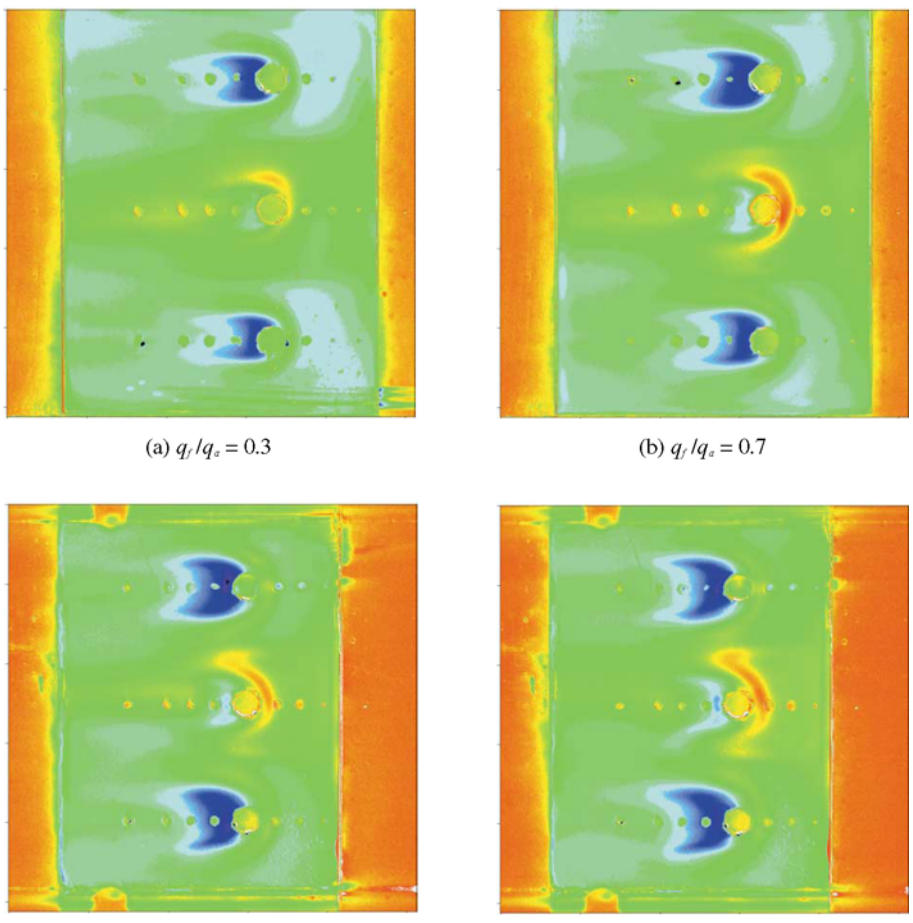

(a) $q_f/q_a = 0.3$ (b) $q_f/q_a = 0.7$

(c) $q_f/q_a = 1.1$ (d) $q_f/q_a = 1.5$

Fig. 7. Visualized oxygen fraction distributions.

When air was injected from the injection nozzles, the pressure in the low-pressure zone rose and began to recirculate. The pressure rose abruptly between $0.5D$ and $1.0D$ upstream of the nozzles, where D is the nozzle diameter, and a horseshoe-shaped area of high pressure was generated in the upper stream of each nozzle. This increase in pressure is caused by a three-dimensional bow shock wave in front of the jet stream. A horseshoe vortex is also created. The three-dimensional bow shock wave bends in the direction of the main stream as it spreads outwards across the width of the flow path, and the wall surface pressure downstream falls drastically. Between the injection nozzles, the tips of the two horseshoe-shaped areas of high pressure interfere with each

other, creating high pressure area that then spreads upstream.

An area of low pressure exists downstream of the side nozzles. This area expands to approximately 2.5D between 0.5D to 1.0D downstream of the nozzle, then settles into a width of 2.0D and splits into two parts. The pressure in the central part of the two-pronged area of low pressure region rises relatively quickly: between 1.0D and 2.0D downstream of the nozzle, the pressure is roughly the same as the surrounding wall pressure.

In Fig. 7, the gas ejected from the central nozzle has been changed from air to oxygen. The dynamic pressure ratio was 0.3 in Fig. 7(a), 0.7 in Fig. 7(b), 1.1 in Fig. 7(c) and 1.5 in Fig. 7(d). In each case, there was a region of high oxygen concentration at the upstream of the central nozzle. There was also a region of high oxygen concentration at the front of the side nozzles, although the concentration was less than that at the central nozzle. This is caused by the influence of the high-pressure region generated by the three-dimensional bow shock wave. The oxygen emitted from the nozzles is caught up in the horseshoe vortex generated by the three-dimensional bow shock wave upstream of the injectors, and flows into the vicinity of the wall in the recirculation region.

Figure 8 shows the oxygen fraction distributions in the recirculation region ((a) Z = 4 mm, (b) Z = 10 mm, (c) Z = 16 mm) along the X-direction. For comparison, Figure 9 shows pressure distributions at Z = 16, 32 and 54 mm along the X-direction when air ejected from all the nozzles at a dynamic pressure ratio of 0.7. The injection nozzles caused no change in the pressure when air was emitted from all the injection nozzles.

As the dynamic pressure ratio increases, the three-dimensional bow shock wave grows stronger and the pressure rises. The oxygen fraction rises with the dynamic pressure ratio. While the pressure distributions at Z = 16 mm are flat, the oxygen fraction distributions are distinctive. From X = ±15 mm, midway point between the injections, the oxygen fraction increases abruptly. There is hardly any mixing from the contact surface of two adjacent flows. Going backwards towards the backward-facing step, this contact surface gradually breaks down and oxygen mixes in with the flows on either side. These facts indicate that each flow creates its own independent vortex in the recirculation zone, and that there is hardly any exchange of gases until the flow becomes mixed in the secondary vortex directly behind the backward-facing step.

The pressure distribution along the X-direction at Z = 32 mm (Fig. 9) suggests that the low pressure area is generated by the separation region downstream of the nozzles. The pressure of the low-pressure area downstream of the central nozzle was slightly higher than that of the two side nozzles. A high-pressure area forms between the nozzles as the horseshoe vortices collide each other. The interference between the wall surface and the horseshoe vortex also forms a high-pressure area in the vicinity of the side wall. The pressure level is roughly equivalent to that of the high-pressure areas between the nozzles.

The oxygen fraction distributions downstream of the injected flow along the X-direction are shown in Fig. 10. The distribution at Z = 32 mm (Fig. 10(a)) suggests that the oxygen fraction near the central nozzle is quite high, and the injected oxygen is caught up in the horseshoe vortex. As the flow convects downstream, the high oxygen fraction caused by the vortex gradually drops, while the oxygen fraction near the central axis rises.

The pressure distribution for Z = 54 mm is shown in Fig. 9. The pressure downstream of the nozzles reaches a maximum value at X = 0 and ±30 mm due to the reattachment of the flow that passes over the horseshoe vortex. In the oxygen fraction distribution at Z = 54 mm, shown in Fig. 10(d), there is a local maximum at X = ±30 mm for each dynamic pressure ratio, but these values are quite small compared with the oxygen fraction at X = 0 mm.

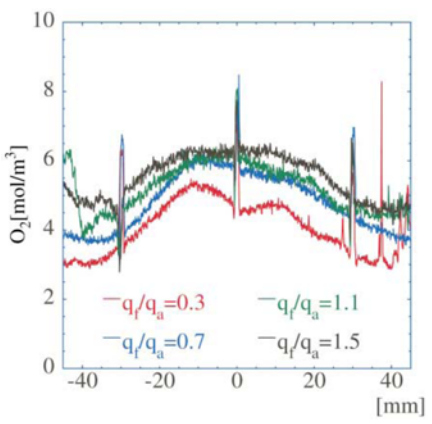

(a) Z = 4 mm

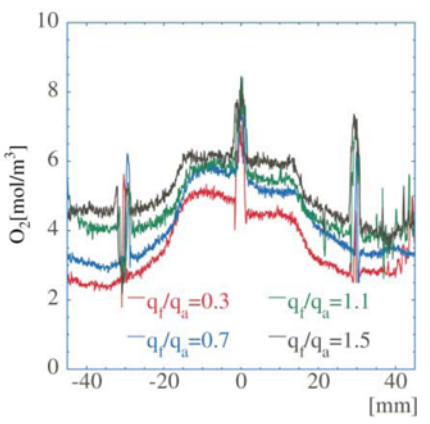

(b) Z = 10 mm

Fig. 8. (continued)

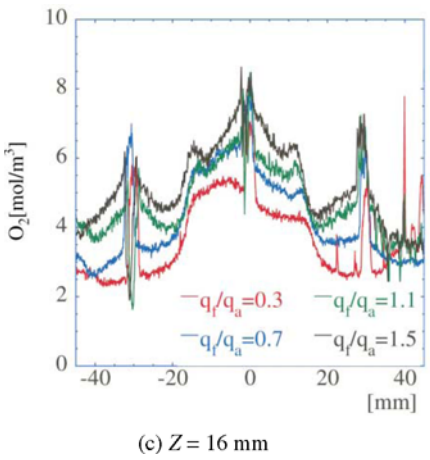

(c) $Z = 16$ mm

Fig. 8. Spanwise oxygen distributions in recirculation region.

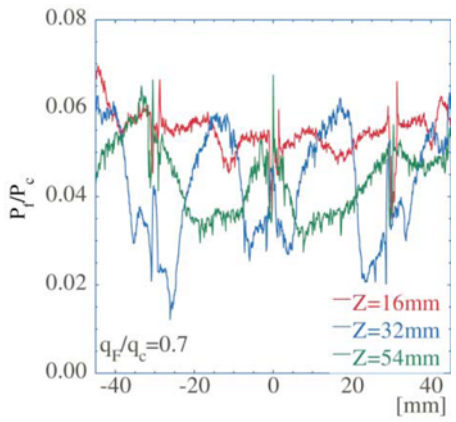

Fig. 9. Spanwise pressure distributions at q_f/q_a = 0.7.

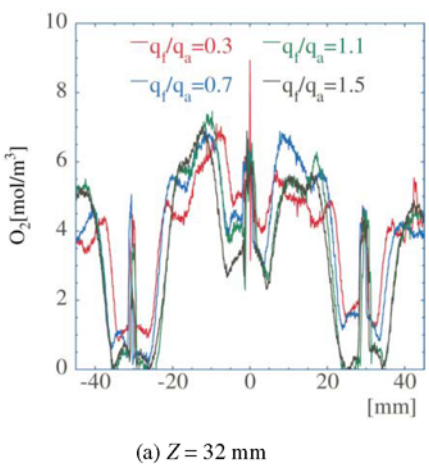

(a) $Z = 32$ mm

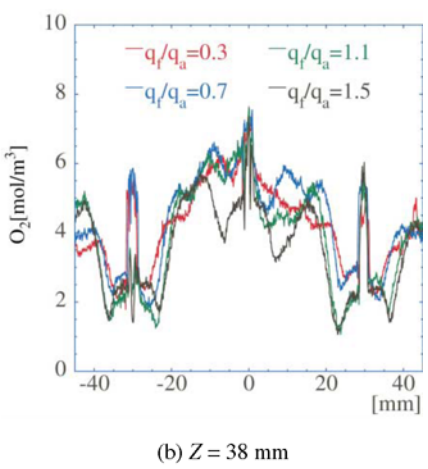

(b) $Z = 38$ mm

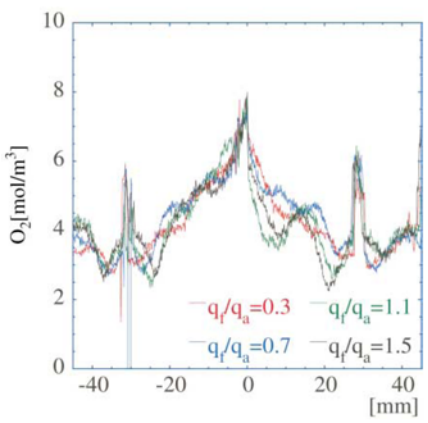

(c) $Z = 44$ mm

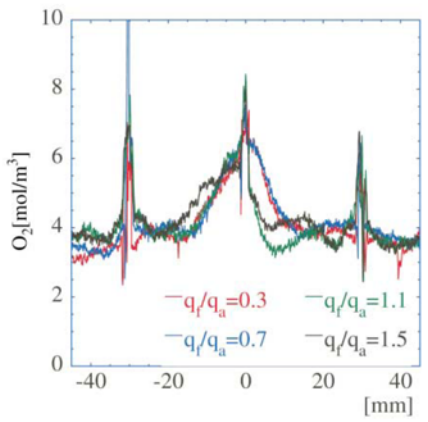

(d) $Z = 54$ mm

Fig. 10. Spanwise oxygen distributions in the downstream of the injectors.

The oxygen fraction local maximum is also caused by the reattachment of flow in this area. High oxygen fraction gas collides with the wall surface, which creates unusually high oxygen fractions.

When the dynamic pressure ratio was increased, the oxygen fraction rose in the recirculation zone and fell in the downstream area. The same trend is observed for the side nozzles that are injecting air. This is because the pressure in the separation zone directly behind the flow falls in proportion to the increase in the dynamic pressure ratio.

5. Conclusions

Pressure sensitive paint was used to measure the wall surface oxygen fraction distributions of the flow field in a supersonic combustor with a backward-facing step. The results provide a more detailed oxygen fraction distributions of the supersonic flow than that obtained by gas sampling ports. PSP is an effective measurement tool that permits investigation of a complicated supersonic flow-mixing field. The conclusions of this study are as follows:

(1) The jet contains its own independent flow structure and little mixing of gases occurs between the flow structures created by each injection nozzle.
(2) The oxygen fraction rises in the recirculation zone when the injection dynamic pressure ratio is increased.
(3) The oxygen fraction falls in the separation zone downstream of the injection nozzles when the injection dynamic pressure ratio is increased.

Acknowledgments

We would like to express our appreciation to Mr. Kuratani and Mr. Niita of Kobe University for their help in carrying out the experiment, to Dr. Teramoto of The Institute of Space and Astronautical Science for his help in processing the PSP image data and to Dr. Handa of Kyushu University and Dr. Sakamura of Toyama Prefectural University for their advice regarding the characteristics of the different types of pressure-sensitive paint.

References

Crites, R. C., Pressure Sensitive Paint Technique, von Karman Institute for Fluid Dynamics Lecture Series 1993-05, (April, 1993), 19-23.

Engler, R. H., Hartmann, K., Troyanovski, I. and Vollan, A., Description and Assessment of a New Optical Pressure Measurement System (OPMS) Demonstrated in the High Speed Wind Tunnel of DLR in Gottingen, DLR-FB (1992), 92-24.

Handa, T., Miyazato, Y., Masuda, M., Matsuo, M., Matsumoto, M. and Sakamoto, K., Experimental Investigation on Luminescent Characteristics of Fast Responding Pressure-Sensitive Paint, Proceedings of PSFVIP-2, (May, 1999), 16-19.

Ikeda, Y., Oyamada, H., Kuratani, N., Nakajima, T., Tomioka, S. and Mitani, T., PIV Measurement of a High-Speed Step Flow with Perpendicular Injection, Collected Papers of the 37th Combustion Symposium (1999), 297-298.

Ito, K., Kido, S., Sakamura, Y., Suzuki, T. and Matsumoto, M., The Application of Pressure Sensitive Paint in Irregular Pressure Fields, 37th Lecture Meeting of the Hokuriku-Shinietsu Branch of The Mechanics Society, (2000).

Tomioka, S., Hiraiwa, T., Mitani, T., Zamma, Y., Shiba, H. and Masuya, G., Auto Ignition in a Supersonic Combustor with Perpendicular Injection behind a Backward-Facing Step, AIAA-97-2889 (1997).

Author Profile

Masashi Matsumoto: He received his B. Sc. (Eng.) degree in Aeronautical Engineering in 1987, and his M.Sc. (Eng.) degree in Aeronautical Engineering in 1989, from Kyushu University. He engaged in Ishikawajima-Harima Heavy Industry Co. Ltd., (IHI) in 1989 as research engineer, and was promoted to acting section manager in 2000. He retired from IHI in 2000. His research interest covers flow visualization and measurement in supersonic flow.

Sadatake Tomioka: He received his B. Sc. (Eng.) degree in Aeronautical Engineering in 1988, and his Dr. (Eng.) degree in Aeronautical Engineering in 1993, from The University of Tokyo. He engaged in The National Aerospace Laboratory of Japan-Kakuda Research Center in 1993 as a researcher, and was promoted to senior researcher in 1998. He worked at Virginia Polytechnic Institute and State University (VA, USA) from 1999 to 2000 as a visiting researcher. His research interest covers mixing and combustion phenomena in supersonic combustors, engine testing and thermodynamics in engines.

Yuji Ikeda: He graduated from Department of Mechanical Engineering, Kobe University (B. Eng., 1984; M. Eng., 1986; Dr. Eng., 1989), and now associate professor. He was a visiting professor of Stanford University from 1994 to 1995. He is a Fellow of Institute of Physics, Chartered Physicist, an editor of "Measurement of Science and Technology" and an AIAA TC member. His research fields are combustion diagnostics, measurement system development, turbulent combustion, spray combustion and discovery science.